ELSEVIER

Materials Science and Engineering A238 (1997) 182–191

MATERIALS SCIENCE & ENGINEERING A

Computer simulation of 90° ferroelectric domain formation in two-dimensions

Hong-Liang Hu *, Long-Qing Chen

Department of Materials Science and Engineering, The Pennsylvania State University, University Park, PA 16802, USA

Abstract

The dynamics of 90° domain formation during a ferroelectric phase transition is studied using a computer simulation model based on time-dependent Ginzburg-Landau (TDGL) equations. This model does not make a priori assumptions on the domain morphologies and their evolution path, and takes into account simultaneously the non-local elastic and electric dipole–dipole interactions, and the local interactions resulting in the domain-wall energy. A two-dimensional system is considered. The domain structure is described by a vector polarization field whose temporal and spatial equation is obtained by numerically solving the TDGL equations in Fourier space. It is shown that both the non-local elastic and electric dipole–dipole interactions are critical in order to explain the experimental observation which demonstrated that tail-to-head or head-to-tail arrangement of dipoles at twin boundaries. © 1997 Elsevier Science S.A.

Keywords: Computer simulation; Ferroelectric domain; Two-dimensional

1. Introduction

Ferroelectric oxide is an important family of ceramics which find applications in capacitors and transducers [1–4]. A common feature to normal ferroelectric ceramics is the formation of domain structures when a paraelectric phase is cooled below the ferroelectric transition temperature. Although the crystallography and thermodynamics of domain structures have been studied quite extensively [2], surprisingly, there have been very few theoretical studies on the kinetics of domain formation as well as the domain evolution under external fields. A fundamental understanding of the domain dynamics is critical for controlling the properties such as permittivity and piezoelectricity [4]. For example, it is critical to understand the evolution of domain structures under external fields in order to control them in poled ferroelectric ceramics for use as piezoelectric transducers.

Many important ferroelectric transitions in oxides are displacive, generating several orientation variants which are related by the symmetry elements of the parent paraelectric phase. For example, in a cubic–tetragonal transformation, there are three possible orientation variants with the tetragonal axes along [100], [010], or [001] directions, or six if we count those along opposite directions as separate variants. The number of orientation variants increases to eight if the crystalline symmetry of the ferroelectric phase is rhombohedral. In the absence of any external field, all of them have the same probability to form in the parent cubic paraelectric phase below the ferroelectric transition temperature. The corresponding microstructure of the ferroelectric phase will contain all possible domains separated by the so-called domain walls. Consequently, in the tetragonal phase it is possible that the polarization vectors in adjacent domains are perpendicular (as in the case of 90° domains) or antiparallel (180° domains) to each other across a domain wall.

Experimentally it is found that 90° domains are predominant in most tetragonal ferroelectrics. In principle, the polarization vectors in adjacent 90° domains can be head-to-tail or head-to-head (tail-to-tail). However, the head-to-head (tail-to-tail) configuration is experimentally shown to be unstable since it results in charged domain walls and consequently has higher electrostatic energy density at the domain boundaries [5].

* Corresponding author. Tel.: + 1 814 863 9957; fax: + 1 814 865 2917.

PII S0921-5093(97)00453-X

The physical origins and the stability of such domain configurations are reasonably understood. There are two types of infinitely long-range interactions involved in ferroelectrics. One is the electric dipole–dipole interactions and the other is the elastic interaction due to the changes in the crystal lattice induced by the displacive transformations. The infinite range nature of those interactions results in a dependence of both the elastic energy and the electrostatic energy on the morphology, shape, distribution and mutual location of domains. Therefore, the domain configuration itself becomes an internal thermodynamic parameter with respect to which the total free energy should be minimized. This is very similar to the case of ferromagnets whose magnetostatic energy depends on the shape, size and mutual location of magnetic domains. A common feature for systems with long-range interactions is the fact that they form modulated domain structures [6]. The typical modulation wavelength is determined by the relative strengths of the short- and long-range interactions. Both the domain structure and the typical wavelength can be modified by applying fields such as stress, magnetic, or electric fields or by changing the temperature. For example, stable 180° domains arise due to the competition between the depolarization energy and the domain wall energy [7]. The domain wall energy prefers a single-domain whereas the depolarization energy prefers opposite alignment of dipoles. For the similar reason, the elastic accommodation between different tetragonal variants leads to the formation of 90° domain structures. The formation of twin lamellae in a single-grain embedded in a polycrystalline ceramics can be understood similar to a coherent precipitate of low symmetry tetragonal phase in a cubic matrix [8–16]. The competition between elastic energy and twin boundary energy results in a polytwin plate consisting of the lamellae of two orientation variants of the low symmetry phase.

As discussed above, our current understanding is mainly limited to the crystallographic and thermodynamic aspects of domain structures, whereas essentially all the experimentally observed domain structures are nonequilibrium. They are frozen domain structures formed along the ferroelectric transformation and subsequent evolution path towards equilibrium. The nonequilibrium domain structures are much more complex and they are difficult to predict analytically. They depend on the initial conditions and they are time-dependent. As a matter of fact, one of the main reasons leading to the difficulties in the commercial production of uniform and consistent materials is that domain structures are time- and history-dependent. Therefore, in order to control the domain structures, it is important that the dynamics of domain formation and evolution be understood. In this paper it will be demonstrated that the Time Dependent Ginsburg-Landau (TDGL) field model will provide us with a powerful framework to address the problem.

In a previous paper [17], a preliminary study of the dynamics of 180° domain formation was reported. It is the purpose of the present paper to extend the study to the more complicated case of 90° domains. The main focus is to investigate the effect of non-local electric dipole dipole interactions on the domain structures. A very similar computer simulation study has been conducted recently by Nambu and Sagala [18] employing TDGL equations. However, they did not take into account the long range electric dipole–dipole interaction, which in fact will be shown in this paper to be essential in predicting the formation of head-to-tail arrangement at the domain walls. Different from [18], we will numerically solve the TDGL equations directly in the Fourier space in which both the elastic and electric dipole–dipole interactions have an analytical form. The elastic energy calculation for both the stress-free and clamped boundary conditions are discussed, although our present simulations were performed for the clamped boundary condition which is believed to be more appropriate for modeling the domain formation in a grain constrained by neighboring grains in a polycrystalline ceramics. One of the main advantages of the TDGL field model is that it does not make a priori assumptions on the domain morphologies and evolution path, and can take into account simultaneously the long-range elastic interaction due to lattice mismatch [8], long range electric dipole–dipole interactions, and the short-range chemical interactions resulting in the domain-wall energy. In the present work, computer simulations were performed in two dimensions (2-D), but the model is also suitable for three-dimensional (3-D) simulation, which will be the subject of a future work. The specific model proposed in this paper corresponds to a cubic–tetragonal phase transition.

This paper is organized as follows: in Section 2, the thermodynamics of domain structures is formulated; Section 3 discusses the elastic strain energy calculation for different boundary conditions; in Section 4, the so-called Time-Dependent Ginsburg-Landau equation is introduced; the results of computer simulation are analyzed in Section 5; finally, the conclusion is contained in Section 6.

2. Thermodynamic description of a domain structure

Landau theory has played an important role in understanding the thermodynamics of ferroelectric phase transitions, for example, the nature or characteristics of a ferroelectric phase transition. For the thermodynamics of a homogeneous system, it is sufficient to consider a free energy density function usually presented as Landau free energy polynomial of order parameters,

which is invariant under the symmetry operation of the parent paraelectric phase. In a ferroelectric phase transition, the primary order parameter is usually the polarization per unit volume. Using this model, the thermodynamic properties and their temperature dependence of the paraelectric phase and a single-domain ferroelectric phase can be predicted. For a ferroelectric phase containing a domain structure is, by definition, an inhomogeneous state in which the polarization is a function of position. Therefore, for modeling the evolution of ferroelectric domains, the spatially dependent polarization field is a natural description of a domain structure. For example, for the particular example of cubic–tetragonal transition, a domain structure is described by a three-component polarization vector field $\boldsymbol{P}=(P_x, P_y, P_z)$. For an inhomogeneous system, the local free energy density also becomes a function of position through the dependence on the polarization vector. Since we are interested in a first-order cubic-to-tetragonal proper ferroelectric transitions, following [19], we employ a six order polynomial for the Landau free energy,

$$\begin{aligned} f_L(P_i) = {} & \alpha_1(P_x^2+P_y^2+P_z^2)+\alpha_{11}(p_x^4+P_y^4+P_z^4) \\ & +\alpha_{12}(P_x^2P_y^2+P_y^2P_z^2+P_z^2P_x^2) \\ & +\alpha_{111}(P_x^6+P_y^6+P_z^6) \\ & +\alpha_{112}(P_x^4(P_y^2+P_z^2)+P_y^4(P_x^2+P_z^2) \\ & +P_z^4(P_x^2+P_y^2))+\alpha_{123}P_x^2P_y^2P_z^2 \end{aligned} \tag{1}$$

where $i, j = 1, 2, 3$ stand for x, y, z, respectively and the α's will be chosen to give the desired equilibrium value of P_i of a single-domain state, i.e. the spontaneous polarization. It can be easily shown that $\alpha_1 = 1/2\varepsilon_0\chi$, where ε_0 is the vacuum permittivity, χ is the susceptibility of the material. If α_1 is negative, the parent paraelectric phase is unstable with respect to the transition to the ferroelectric phase, and if it is positive, the initial paraelectric phase is metastable. To describe a first order transition, α_{11} has to be negative. In the ferroelectric state, the vector field takes one of the six states $\boldsymbol{P}=P_0(1,0,0)$, $P_0(-1,0,0)$, $P_0(0,1,0)$, $P_0(0,-1,0)$, $P_0(0,0,1)$, $P_0(0,0,-1)$, where P_0 is the spontaneous polarization at a given temperature.

Across the boundaries between different ferroelectric domains, the values of the polarization field are different from the bulk equilibrium values and depend on the plane and orientation of the boundary plane. It is assumed that they vary continuously across the domain boundaries. In the Ginzburg-Landau free energy model, the domain wall energy is introduced through gradients of the polarization field. For a cubic system [20],

$$\begin{aligned} f_G(P_{i,j}) = {} & \tfrac{1}{2}G_{11}(P_{x,x}^2+P_{y,y}^2+P_{z,z}^2) \\ & +G_{12}(P_{x,x}P_{y,y}+P_{y,y}P_{z,z}+P_{z,z}P_{x,x}) \\ & +\tfrac{1}{2}G_{44}((P_{x,y}+P_{y,x})^2+(P_{y,z}+P_{z,y})^2+(P_{z,x}+P_{x,z})^2) \\ & +\tfrac{1}{2}G'_{44}((P_{x,y}-P_{y,x})^2+(P_{y,z}-P_{z,y})^2+(P_{z,x}-P_{x,z})^2) \end{aligned} \tag{2}$$

where $P_{i,j}=\partial P_i/\partial x_j$. It is clear that for a generic choice of G_{11}, G_{12}, G_{44}, and G'_{44}, the domain wall energy is not isotropic.

Cubic–tetragonal displacive phase transitions are structural transformations involving a change of crystal structures and lattice parameters. If we assume that the boundaries between the parent paraelectric phase and the product ferroelectric phase as well as the boundaries between the different orientation domains of the ferroelectric phase are coherent, elastic strain energy will be generated during the phase transition in order to accommodate the structural changes. We assume that the local elastic strain generated during the phase transition has a linear-quadratic coupling with the local polarization field. This coupling results in the so-called electrostrictive energy

$$\begin{aligned} f_{es}(P_i, \eta_{ij}) = {} & -q_{11}(\eta_{xx}P_x^2+\eta_{yy}P_y^2 \\ & +\eta_{zz}P_z^2)-q_{12}(\eta_{xx}(P_y^2+p_z^2)+\eta_{yy}(P_x^2+P_z^2) \\ & +\eta_{zz}(P_x^2+P_y^2))-2q_{44}(\eta_{xy}P_xP_y+\eta_{xz}P_xP_z+\eta_{yz}P_yP_z) \end{aligned} \tag{3}$$

where q_{ij} are the electrostrictive constants and $\eta_{ij}=1/2(u_{i,j}+u_{j,i})$ is the linear elastic strain, u_i is elastic displacement. The corresponding elastic energy density reads

$$\begin{aligned} & f_{ela}(\eta_{ij}) \\ & = \tfrac{1}{2}C_{11}(\eta_{xx}^2+\eta_{yy}^2+\eta_{zz}^2)+C_{12}(\eta_{xx}\eta_{yy}+\eta_{yy}\eta_{zz}+\eta_{zz}\eta_{xx}) \\ & \quad +2C_{44}(\eta_{xy}^2+\eta_{yz}^2+\eta_{zx}^2) \end{aligned} \tag{4}$$

where C_{ij}'s are the second-order elastic constants.

And finally, for an inhomogeneous system, we have to consider the long range electric dipole–dipole interactions. In SI units, it takes the familiar form

$$F_{dip}P_i = \frac{1}{8\pi\varepsilon_0\chi}\int\int d^3\mathbf{r}_i d^3\mathbf{r}_j\left(\frac{\boldsymbol{P}(\mathbf{r}_i)\cdot\boldsymbol{P}(\mathbf{r}_j)}{|\mathbf{r}_i-\mathbf{r}_j|^3} - \frac{3(\boldsymbol{P}(\mathbf{r}_i)\cdot(\mathbf{r}_i-\mathbf{r}_j))\,(\boldsymbol{P}(\mathbf{r}_j)\cdot(\mathbf{r}_i-\mathbf{r}_j))}{|\mathbf{r}_i-\mathbf{r}_j|^5}\right) \tag{5}$$

where χ is the dielectric susceptibility of the material. We will see that it is this interaction which is responsible to the head-to-tail arrangement of dipoles at the twin boundaries.

In summary, the total free energy of a system with a domain structure is the sum of the Landau bulk free energy F_L, the gradient energy F_G, the electrostrictive energy F_{es}, the elastic energy F_{ela}, and the energy due to the long range electric dipole–dipole interaction

$$
\begin{aligned}
&F(P_i, P_{i,j}, \eta_{ij}) \\
&= F_L P_i + F_G P_{i,j} + F_{es}(P_i, \eta_{ij}) + F_{ela}\eta_{ij} + F_{dip}P_i \\
&= \int d^3r\,[f_L(P_i) + f_G(P_{i,j}) + f_{es}(P_i, \eta_{ij}) + f_{ela}(\eta_{ij})] + \overline{F_{dip}}P_i
\end{aligned} \tag{6}
$$

It should be pointed out that although the elastic strain energy which appears in the total free energy Eq. (6) as a volume integral of an elastic strain energy density function, minimization of the total free energy with respect to elastic strain immediately results in non-local elastic interactions between the volume elements of a domain structure described by a nonequilibrium polarization field.

3. The elastic strain energy of a domain structure

In the model given in the previous section, both the polarization field and the linear elastic strain field appear to be order parameters. However, it is commonly accepted that the mechanical relaxation of elastic field is much faster than the electric relaxation of polarization field. Consequently, we can assume that during the process of ferroelectric transition, the system in question reaches its mechanical equilibrium instantaneously at every stage. By eliminating the elastic strain field using the static condition of mechanical equilibrium, the elastic strain energy of a domain structure becomes only a functional of the polarization field.

It is easy to see that for a stress-free homogeneous system, minimization of the total free energy with respect to the elastic strain results in a simple renormalization of the constants α_{11} and α_{12} in front of the fourth order term in the Landau free energy. This renormalization usually produces a stronger first-order phase transition.

For an inhomogeneous system, let us write the elastic strain field as a sum of a spatially independent homogeneous strain, $\bar{\eta}_{i,j}$, and a spatially-dependent heterogeneous strain field $\delta\eta_{i,j}$. The homogeneous strain determines the macroscopic shape deformation of the crystal as a whole produced by internal stress due to the presence of domain structures. The heterogeneous strain is defined in such a way that

$$\int \delta\eta_{i,j}\, d^3r = 0 \tag{7}$$

If there is no external stress applied and the crystal is unconstrained with respect to the macroscopic deformation, the equilibrium deformation due to the formation of a given domain structure is obtained by minimizing the total energy of the system with respect to the homogeneous strain,

$$
\begin{aligned}
\bar{\eta}_{xx} &= Q_{11}\overline{P_x^2} + Q_{12}(\overline{P_y^2} + \overline{P_z^2}) \\
\bar{\eta}_{yy} &= Q_{11}\overline{P_y^2} + Q_{12}(\overline{P_x^2} + \overline{P_z^2}) \\
\bar{\eta}_{zz} &= Q_{11}\overline{P_z^2} + Q_{12}(\overline{P_x^2} + \overline{P_y^2}) \\
\bar{\eta}_{yz} &= (q_{44}/(2C_{44}))\overline{P_yP_z} \\
\bar{\eta}_{xz} &= (q_{44}/(2C_{44}))\overline{P_xP_z} \\
\bar{\eta}_{xy} &= q_{44}/(2C_{44}))\overline{P_xP_y}
\end{aligned} \tag{8}
$$

where $\overline{P_i^2}$ and $\overline{P_iP_j}$ represent the volume averages over a system containing domain structures, and

$$
\begin{aligned}
Q_{11} &= \frac{1}{3}\left[\frac{q_{11}+2q_{12}}{C_{11}+2C_{12}} + 2\frac{q_{11}-q_{12}}{C_{11}-C_{12}}\right] \\
Q_{12} &= \frac{1}{3}\left[\frac{q_{11}+2q_{12}}{C_{11}+C_{12}} - \frac{q_{11}-q_{12}}{C_{11}-C_{12}}\right]
\end{aligned} \tag{9}
$$

The elastic energy and electrostrictive energy due to the homogeneous deformation can be obtained by substituting the equilibrium homogeneous strain (Eq. (8)) back to the elastic strain energy expression f_{ela} and the electrostrictive energy expression f_{es}, respectively. It is easy to see that they depend on the volume fractions of each orientation domain. On the other hand, if the boundary is clamped instead of stress-free, the homogeneous deformation is prohibited and the corresponding homogeneous strain is zero.

The equilibrium heterogeneous strain field $\delta\eta_{i,j}$ satisfies the mechanical equilibrium condition given by the Euler equation with respect to the elastic displacement:

$$\sigma_{ij,j} = 0, \quad (i, j = 1, 2, 3) \tag{10}$$

where

$$\sigma_{ij} = \frac{\partial F}{\partial \eta_{ij}} \tag{11}$$

is the Cauchy stress tensor, F is the total free energy functional.

For the case of homogeneous modulus approximation, the equilibrium Eq. (10) can be readily solved in the Fourier space. Details of the derivation can be found in [8] and [18]. The sum of elastic strain energy and the electrostrictive energy due to the heterogeneous strain relaxation is given by

$$F_{het} = -\frac{1}{2}\int \frac{d^3k}{(2\pi)^3}(n_i\Gamma_{ij}(\boldsymbol{k})\Omega_{jl}(\boldsymbol{n})\Gamma^*_{lm}(\boldsymbol{k})n_m) \tag{12}$$

where $\boldsymbol{n} = (n_1, n_2, n_3)$, $n_i = k_i/|\boldsymbol{k}|\,(i = 1, 2, 3)$ is the unit vector in the reciprocal space. $\Gamma_{ij}(\boldsymbol{k})$ are Fourier transformation of $\Gamma_{ij}(\boldsymbol{r})$, which in turn are given by

$$
\begin{aligned}
\Gamma_{11} &= q_{11}P_x^2 + q_{12}(P_y^2 + P_z^2), \\
\Gamma_{22} &= q_{11}P_y^2 + q_{12}(P_x^2 + P_z^2), \\
\Gamma_{33} &= q_{11}P_z^2 + q_{12}(P_x^2 + P_y^2), \\
\Gamma_{12} &= \Gamma_{21} = 2q_{44}P_xP_y, \\
\Gamma_{23} &= \Gamma_{32} = 2q_{44}P_yP_z, \\
\Gamma_{31} &= \Gamma_{13} = 2q_{44}P_xP_z.
\end{aligned} \tag{13}
$$

Table 1
Values of effective coefficients used in the simulation

α'_{11}	α'_{12}	α'_{111}	α'_{112}	g_{14}	g_{44}	q'_{11}	q'_{12}	q'_{44}	C'_{11}	C'_{12}	C'_{44}
−0.5	9.0	0.8	4.0	0.0	1.0	2.2	−0.9	0.58	2.75	1.79	0.54

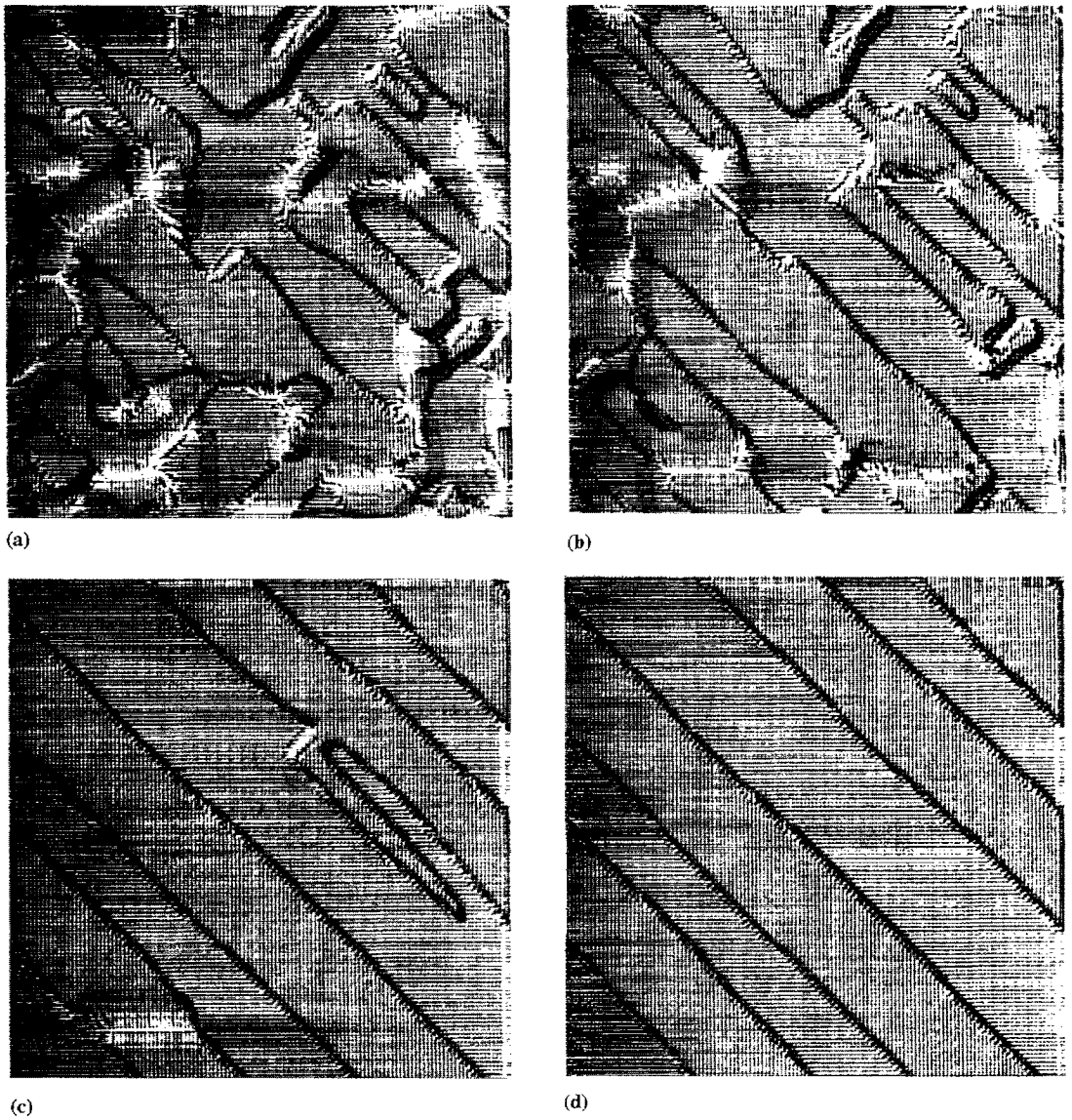

Fig. 1. Domain evolution in the presence of both dipole–dipole and elastic interactions. (a) 2500 Time steps; (b) 5000 steps; (c) 12 500 steps; (d) 25 000 steps.

Ω_{jm} is given by

$$\Omega_{ii}(n) = \frac{C_{44} + (C_{11} - C_{44})(n_j^2 + n_k^2) + \zeta(C_{11} + C_{12})n_j^2 n_k^2}{C_{44}D(n)}$$

$$\Omega_{ij}(n) = -\frac{(C_{12} + C_{44})(1 + \zeta n_k^2)}{C_{44}D/(n)} n_i n_j, \qquad (14)$$

where indices i, j, k form a cyclic sequence

$$\zeta = (C_{11} - C_{12} - 2C_{44})/C_{44} \qquad (15)$$

is the elastic anisotropy and

$$D(\boldsymbol{n}) = C_{11} + \zeta(C_{11} + C_{12})(n_2^1 n_2^2 + n_1^2 n_3^2 + n_2^2 n_3^2) + \zeta^2(C_1 + 2C_{12} + C_{44})n_1^2 n_2^2 n_3^2 \qquad (16)$$

It can be easily shown that by converting the expression for the elastic strain energy and the electrostrictive energy Eq. (12) from Fourier space to the real space, the elastic interactions are non-local and highly anisotropic.

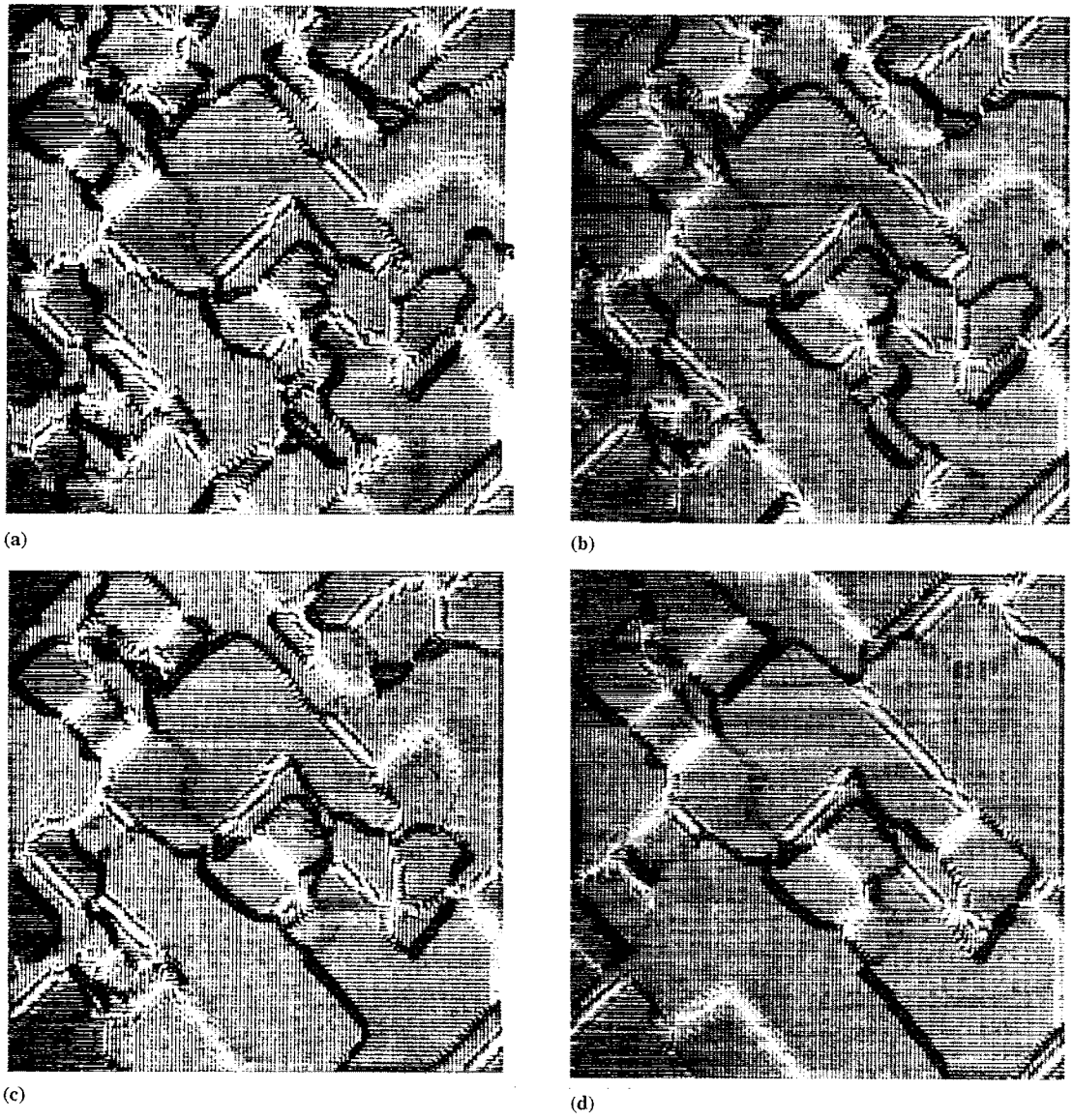

Fig. 2. Domain evolution in the presence of elastic interaction but the absence of dipole–dipole interaction. (a) 5000 Steps; (b) 10 000 steps; (c) 25 000 steps; (d) 50 000 step.

4. The domain evolution equation

The three components of the polarization vector represent three non-conserved order parameter fields since the volume fraction of each orientation domain is not constant during the evolution of domain structure. The temporal relaxation of non-conserved fields is described by the TDGL equations [21], i.e.

$$\frac{\partial}{\partial t} P_i(r, t) = -L \frac{\partial F'}{\partial P_i(r, t)} + \xi_i(r, t) \tag{17}$$

where F' is the total free energy functional after eliminating the elastic field, $\xi_i(r, t)$ is the Gaussian random fluctuation satisfying

$$\langle \xi_i(r, t) \rangle = 0$$
$$\langle \xi_i(r, t)\xi_j(r', t') \rangle = 2k_B TL\delta_{ij}\delta(r - r')\delta(t - t'). \tag{18}$$

where k_B is the Boltzman constant, T is temperature, δ_{ij} is the Kronecker symbol, and $\delta(r-r')$ is the Delta function. The bracket $< .. >$ denotes an average over fluctuations of all the $\xi_i(r, t)$.

5. Computer simulation results and discussion

The temporal evolution of the polarization vector fields, and thus the domain structures, is obtained by numerically solving the TDGL equations. Since the elastic strain energy and the electrostrictive energy due to the heterogeneous strain field have a single analytical expression as a functional of the polarization field in

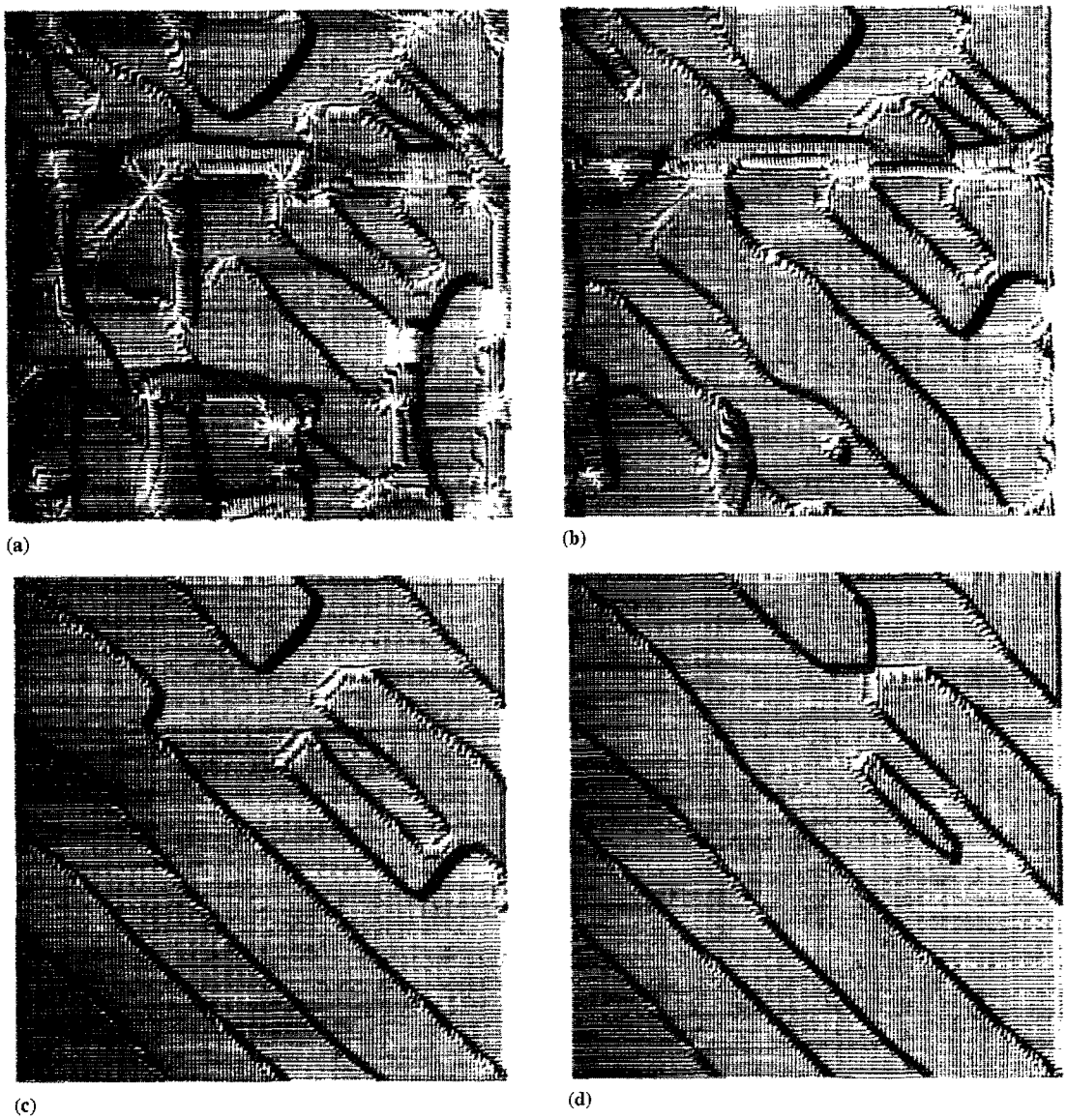

Fig. 3. Domain evolution in the presence of dipole–dipole interaction but the absence of elastic interaction. (a) 2500 Steps; (b) 5000 steps; (c) 12 500 steps; (d) 25 000 steps.

Fourier space, the computer simulation is most convenient to be performed directly in the reciprocal space. It is straightforward to transform the bulk Landau free energy term and the gradient term to the reciprocal space, while there is some subtlety in transforming the dipole–dipole interaction term. The result is

$$F_{\mathrm{dip}} = \frac{1}{8\pi\varepsilon_0\chi}\int\int d^3\boldsymbol{r}_i d^3\boldsymbol{r}_j\left(\frac{\boldsymbol{P}(\boldsymbol{r}_i)\cdot\boldsymbol{P}(\boldsymbol{r}_j)}{|\boldsymbol{r}_i-\boldsymbol{r}_j|^3} - \frac{3(\boldsymbol{P}(\boldsymbol{r}_i)\cdot(\boldsymbol{r}_i-\boldsymbol{r}_j))(\boldsymbol{P}(\boldsymbol{r}_j)\cdot(\boldsymbol{r}_i-\boldsymbol{r}_j))}{|\boldsymbol{r}_i-\boldsymbol{r}_j|^5}\right)$$
$$= \frac{1}{2\pi\varepsilon_0\chi}\int\frac{d^3\boldsymbol{k}}{(2\pi)^3}\frac{|\boldsymbol{P}(\boldsymbol{k})\cdot\boldsymbol{k}|^2}{k^2} = \frac{1}{2\pi\varepsilon_0\chi}\int\frac{d^3\boldsymbol{k}}{(2\pi)^3}|\boldsymbol{P}(\boldsymbol{k})\cdot\boldsymbol{n}|^2 \tag{19}$$

where

$$\boldsymbol{P}(\boldsymbol{k}) = \int\frac{d^3\boldsymbol{r}}{(2\pi)^3}\boldsymbol{P}(\boldsymbol{r})e^{-i\boldsymbol{k}\cdot\boldsymbol{r}} \tag{20}$$

is the Fourier transform of the polarization field $P(\boldsymbol{r})$.

It is easily shown that at $\boldsymbol{k}=0$, $(\boldsymbol{P}(\boldsymbol{k})\cdot\boldsymbol{n})^2$ is undefined. In this work the $\boldsymbol{k}=0$ point was excluded in the computation. For a homogeneous system, we consider the dipole–dipole interaction energy has been incorporated in the Landau free energy. For an inhomogeneous system, at $\boldsymbol{k}=0$, $\boldsymbol{P}(\boldsymbol{k}=0)=\int d^3\boldsymbol{r}\boldsymbol{P}(\boldsymbol{r})$ is the total polarization in the entire system. When the domain size is much smaller than the system size and in the absence of an external electric field, it is reasonable to assume that the volume average of polarization field is zero in the multiple domain case. As a result, the

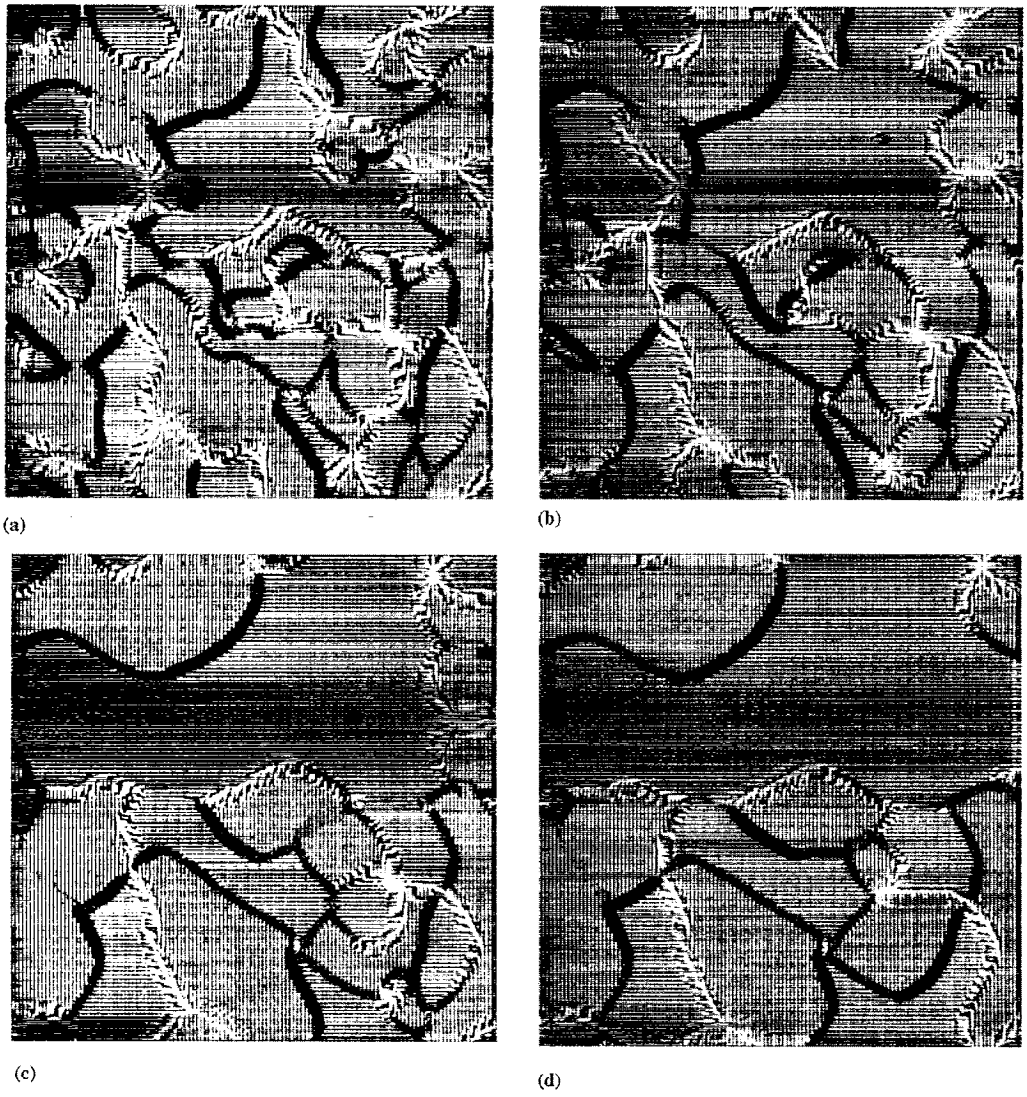

Fig. 4. Domain evolution in the absence of elastic and dipole–dipole interactions. (a) 5000 Steps; (b) 10 000 steps; (c) 25 000 steps; (d) 50 000 steps.

contribution from the $k = 0$ point to F_{dip} is automatically zero. However, if the domain size is comparable to the system size, the $k = 0$ point becomes important. Excluding the $k = 0$ is equivalent to excluding the depolarization field arising from the surfaces of a system of finite size. In the current simulation, periodic boundary conditions are applied and therefore there is no depolarization field due to external surfaces.

Of course, in Fourier-transforming the TDGL equation, one has to transform $\delta F/\delta P_i$ instead of F to the reciprocal space.

In the present work, the TDGL equations in the reciprocal space are solved using the simple forward Euler technique. As a first step, computer simulations are performed in two dimensions. We employ a 128×128 lattice with periodic boundary conditions along both Cartesian axes. We consider only the clamped boundary condition in which the homogeneous strain is zero. The back-Fourier transform at a given step produces the real-space domain structures represented by the polarization fields. Since we work in two dimensions, the polarization vector field has two components. To further simplify the problem, the noise term is also neglected.

In the simulation, we employ a set of the dimensionless variables. Since α_1, L and G_{11} have units of $C^{-2}\,m^2\,N$, $s^{-1}\,m^{-2}\,C^2\,N^{-1}$ and $C^{-2}\,m^4\,N$ [22], respectively, it is clear that $\sqrt{G_{11}/|\alpha_1|}$ and $1/(|\alpha_1|L)$ have the dimensions of distance and time, respectively. So a natural choice of the dimensionless reduced variables is:

$$\begin{aligned} \hat{r} &= \sqrt{|\alpha_1|/G_{11}}\,r\,, \\ \tau &= |\alpha_1|Lt\,, \\ \hat{P} &= P/|P_0|\,. \end{aligned} \tag{21}$$

Where $\boldsymbol{P}_0$ is the spontaneous polarization at a given temperature. In the reduced variables, the effective coefficients are related to the original ones as follows:

$$\begin{aligned}
&\alpha'_1 = \alpha_1/|\alpha_1|\,,\\
&\alpha'_{11} = \alpha_{11}P_0^2/|\alpha_1|\,,\\
&\alpha'_{12} = \alpha_{12}P_0^2/|\alpha_1|\,,\\
&\alpha'_{111} = \alpha_{111}P_0^4/|\alpha_1|\,,\\
&\alpha'_{112} = \alpha_{112}P_0^4/|\alpha_1|\,,\\
&g_{14} = (G_{11} + G_{44} - G'_{44})/G_{11}\,,\\
&g_{44} = (G_{44} + G'_{44})/G_{11}\,,\\
&q'_{11} = q_{11}/|\alpha_1|\,,\\
&q'_{12} = q_{12}/|\alpha_1|\,,\\
&q'_{44} = q_{44}/|\alpha_1|\,,\\
&C'_{11} = C_{11}/(|\alpha_1|P_0^2)\,,\\
&C'_{12} = C_{12}/(|\alpha_1|P_0^2)\,,\\
&C'_{44} = C_{44}/(|\alpha_1|P_0^2)\,,
\end{aligned} \tag{22}$$

where $P_0 = |\boldsymbol{P}_0|$. It is clear that $\alpha'_1 = -1.0$. In reduced variables, the lattice spacing in real space is chosen to be $\Delta x = 0.5$, the time step is $\Delta\tau = 0.01$. The values of other coefficients used in our simulation are given in Table 1.

It should be noted that, in our simulation the gradient energy coefficients are chosen in such a way to provide the isotropic domain wall energy.

Fig. 1 shows an example of formation of a domain structure and its subsequent temporal evolution. The initial condition is a high-temperature homogeneous paraelectric phase, created by assigning a zero value at each lattice site for both components of the polarization field. In Fig. 1, the magnitude and direction of the local electric polarization field are represented by the length and the arrow direction of short-lines. Since the coefficient, α_1 in the Landau free energy expression is chosen to be negative, the initial paraelectric phase is unstable with respect to the transition to the ferroelectric phase, and hence small random perturbation introduced to the initial uniform paraelectric state is sufficient to trigger the transition. It can been seen in Fig. 1, that during the initial stages of domain coarsening after the system is transformed to the ferroelectric state, all four (six in three dimensions) different kinds of orientation domains allowed by symmetry are present. Clearly, there is quite strong alignment of domain walls along the [11] directions of the two-dimensional lattice. Since in this case, the gradient energy coefficients are chosen in such a way that the domain wall energy is isotropic, the domain wall alignment must be entirely due to the anisotropic and non-local elastic and electric dipole–dipole interactions. Indeed, as shown in Fig. 2, the domain structure is visually isotropic if both the elastic and electric dipole–dipole interactions are removed.

One may also notice in Fig. 1a that both head-to-head and tail-to-tail arrangements of polarization fields across the domain walls are present. As time increases, the fraction of head-to-head and tail-to-tail domain walls decreases (Fig. 1(b–c)). Eventually, as shown in Fig. 1d, only those domain walls with the head-to-tail arrangement survive. However, as shown in Fig. 3, by excluding the electric dipole–dipole interactions, there exist many head-to-head and tail-to-tail domain walls even after much longer simulation time than in the case described in Fig. 1. By comparing Fig. 1 and Fig. 3, it also seems to be true that the electric dipole–dipole interactions result in faster domain growth as a result of the dramatic increase in the energies of domain walls with head-to-head and tail-to-tail configurations, and thus, their faster elimination compared with head-to-tail domain walls. Our calculation shows that the domain wall energy with either head-to-head or tail-to-tail arrangement is about two orders of magnitude higher than the head-to-tail configurations.

It is also interesting to find that even when the elastic energy term is absent, the electrical dipole–dipole interactions produce strong alignment along the [11] directions, indicating that the minimization of dipole–dipole interactions prefer the [11] domain wall orientation in a multidomain system.

It should be emphasized that our simulations were performed using periodic boundary conditions and under the constrained condition under which the homogeneous strain relaxations are not allowed. Different boundary conditions may lead to different domain structures and their evolution path, Fig. 4.

In the present work, the computer simulation is performed in 2D. It is desirable to extend the work to 3D since in this case there is one more dimension to relax the free energy and as a result more complicated domain structures can develop. We want to stress that the model developed here is suitable for 3D simulation. Indeed, we expect to be able to report the results of 3D simulation based on the present model in the near future.

The effect of random thermal noise is neglected in this work, in the belief that at low temperature thermal noise plays little role in the late stage of the domain evolution. However, to better understand the formation of twin structures in the ferroelectric transition, it is essential to include the thermal noise term to simulate the nucleation process. Furthermore, in this paper, we considered the case in which the paraelectric phase is unstable with respect to the ferroelectric phase transition. It will be interesting to study the nucleation mechanism when the parent phase is metastable.

6. Summary

In conclusion, a computer simulation model for 90° ferroelectric domain formation and evolution is developed, based on the TDGL equations. Long range electric dipole–dipole interactions, long range elastic interactions and short range chemical interactions are taken into account simultaneously. Various effects of these interactions are discussed. It is found that to account for the formation of head-to-tail arrangements of dipoles at the domain boundaries, it is essential that the dipole–dipole interaction be included.

Acknowledgements

The authors are grateful for the fruitful discussions with A.G. Khachaturyan and for the financial support of NSF under the grant number DMR 96-33719.

References

[1] M.E. Lines, A.M. Glass, Principles and Applications of Ferroelectrics and Related Materials, Clarendon Press, Oxford, 1977.
[2] Special Issue on Domain Structures in Ferroelectrics, Ferroelastics and Other Ferroic Materials, Part I and Part II Ferroelectrics (1989) 97–98.
[3] J.C. Burfoot, G.W. Taylor, Polar Dielectrics and Their Applications, MacMilan, London, 1979.
[4] L.E. Cross, in: Ferroelectric Ceramics, Birkhauser Verlag, Basel, Switzerland, 1992.
[5] C.A. Randall, D.J. Barber, R.W. Whatmore, J. Mater. Sci 22 (1987) 925.
[6] M. Seul, D. Andelman, Science 267 (1995) 476.
[7] T. Mitsui, J. Furuichi, Phys. Rev. 90 (1953) 153.
[8] A.G. Khachaturyan, Theory of Structural Transformations in Solids, Wiley, New York, 1983.
[9] D.R. Clarke, Metall. Trans. A 7A (1976) 723.
[10] A.L. Roitburd, Solid State Physics, Academic Press New York, 33, 1978, pp. 317.
[11] K.S. Sree Harsha, Metall. Trans. A 21A (1983) 365.
[12] J.K. Lee, M.H. Yoo, Metall. Trans. A. 21A (1992) 2999.
[13] G. Arlt, J. Mater. Sci. 25 (1990) 2655.
[14] P. Xu, J.W. Morris Jr., Metall. Trans. A 23A (1992) 2999.
[15] G.R. Barsch, J.K. Krumhansl, Phys. Rev. Lett. 53 (1984) 1069.
[16] B. Horovitz, G.R. Barsch, J.A. Krumhansl, Phys. Rev. B43 (1991) 1032.
[17] W. Yang, L.Q. Chen, J. Am. Ceram. Soc. 78 (1995) 2554.
[18] S. Nambu, D.A. Sagala, Phys. Rev. B50 (1994) 5838.
[19] A.F. Devonshire, Advances in Phys. 3 (1954) 85; A.F. Devonshire, Philos. Mag. 40 (7) (1949) 1040; Philos. Mag. 42 (7) (1951) 1065; see also: E. Fatuzzo, W.J. Merz, Ferroelectricity (North-Holland, Amsterdam; Wiley, New York, 1967).
[20] W. Cao, L.E. Cross, Phys. Rev. B44 (1991) 5.
[21] J.D. Gunton, M. San Miguel, P.S. Sahni, in: C. Domb, J.L. Lebowitz (Eds.), Phase Transitions and Critical Phenomena, Academic, New York, 1983, Vol. 8.
[22] K.H. Hellwege, A.M. Hellwege (Eds.), Elastic, Piezoelectric, Pyroelectric, Electrooptic Constants, and Nonlinear Dielectric Susceptibilities of Crystals, Landolt-Borstein, New Series, Group 3, Vol. 11 Springer-Verlag, Berlin, 1979; K.H. Hellwege, A.M. Hellwege (Eds.), Ferroelectrics and Related Substances, Landolt-Borstein, New Series, Group 3, Vol. 16, Pt. A, Springer-Verlag, Berlin, 1982.